Submitted: 10 October, 2025 Accepted: 16 December, 2025 Published: 30 April, 2026 DOI:10.22514/jomh.2026.033

ORIGINAL RESEARCH

JOMH Journal of Men's Health

ALYREF correlates with tumor progression and therapy resistance in localized and advanced prostate cancer

Zhouda Cai[1,†], Yu Liu[2,†], Shengda Song[3], Chuanfan Zhong[1], Jiahong Chen[4], Le Zhang[5], Chao Cai[2], Jianming Lu[1], Yanru Zeng[1,6,*], Weide Zhong[1,2,*]

[1]Department of Urology, Guangdong Key Laboratory of Clinical Molecular Medicine and Diagnostics, Guangzhou First People's Hospital, Guangzhou Medical University, 510180 Guangzhou, Guangdong, China
[2]Department of Urology, Minimally Invasive Surgery Center, The First Affiliated Hospital of Guangzhou Medical University, Guangdong Key Laboratory of Urology, Guangzhou Institute of Urology, 510230 Guangzhou, Guangdong, China
[3]Department of Urology, Meizhou People's Hospital (Huangtang Hospital), 514000 Meizhou, Guangdong, China
[4]Department of Urology, Huizhou Central People's Hospital, 516000 Huizhou, Guangdong, China
[5]Institute for Integrative Genome Biology, University of California, Riverside, CA 92507, USA
[6]Institute of Gerontology, Guangzhou Geriatric Hospital, Guangzhou Medical University, 510550 Guangzhou, Guangdong, China

***Correspondence**
eyweidezhong@scut.edu.cn (Weide Zhong);
Jolene@gzhmu.edu.cn (Yanru Zeng)

† These authors contributed equally.

Abstract

Background: Prostate cancer (PCa) is a leading malignancy in men, with a poor prognosis in the advanced stage. Aly/REF export factor (*ALYREF*), a 5-methylcytosine (m5C)-binding protein regulating RNA export, has been implicated in several cancers. This study aimed to clarify the role of *ALYREF* in PCa progression and prognosis. **Methods**: We integrated multi-omics datasets from The Cancer Genome Atlas (TCGA), Stand Up To Cancer (SU2C), Genotype-Tissue Expression (GTEx), and Cancer Dependency Map (DepMap) with immunohistochemistry and *in vitro* assays. Survival outcomes were analyzed using Kaplan-Meier and Cox regression. Functional enrichment assessed *ALYREF*-associated pathways, while *ALYREF* knockdown in LNCaP and enzalutamide-resistant cells evaluated its oncogenic role. **Results**: *ALYREF* was significantly upregulated in multiple cancer types and correlated with poor prognosis in PCa. High *ALYREF* expression predicted biochemical recurrence in localized PCa and shorter progression-free and overall survival in advanced PCa. Multi-omics profiling revealed enrichment in MYC targets, oxidative phosphorylation, E2F signaling, and mTORC1 pathways. DepMap data showed that *ALYREF* is essential for tumor cell proliferation, with high dependency in PCa lines. Consistently, *ALYREF* knockdown suppressed cell viability and clonogenic growth in both hormone-sensitive and resistant models. **Conclusions**: This study identifies *ALYREF* as an oncogenic driver and unfavorable prognostic biomarker in PCa. Integrating multi-omics evidence with functional validation, *ALYREF* emerges as a promising therapeutic target, particularly in advanced and therapy-resistant PCa.

Keywords

ALYREF; Prostate cancer; Biomarkers; Multi-omics analysis

1. Introduction

Prostate cancer (PCa) ranks as the second most common malignancy among men globally and is the most prevalent malignant tumor in elderly men, with its mortality rate ranking fifth among cancers affecting men worldwide [1]. Over recent decades, advancements in diagnostic technologies and therapeutic approaches have significantly improved the overall survival rates of PCa patients [2]. PCa is an androgen-dependent disease, and current treatment options for early-stage PCa include surgical resection and radical radiotherapy [3]. However, a subset of patients inevitably progresses from hormone-sensitive prostate cancer to an advanced stage known as castration-resistant prostate cancer (CRPC). Once PCa advances to CRPC, the standard first-line treatment shifts to androgen deprivation therapy (ADT) combined with drugs targeting androgen receptor (AR) signaling pathways [4]. While significant progress has been made in the treatment of localized PCa globally, the prognosis for advanced PCa remains poor, with a substantial proportion of male patients succumbing to the disease [5]. Consequently, the identification of novel biomarkers and therapeutic targets is urgently needed to develop personalized treatment strategies for PCa patients [6].

Nonmutational epigenetic reprogramming represents a critical hallmark of tumor heterogeneity [7]. Among various RNA modifications, RNA 5-methylcytosine (m5C), characterized by the methylation of the fifth carbon of cytosine in RNA, plays a pivotal role in this process [7]. The regulation of RNA m5C is orchestrated by a suite of proteins, including methyltransferases ("writers"), demethylases ("erasers"), and RNA-binding proteins ("readers"), which collectively modulate the dynamic m5C modification landscape [8]. Prior studies have demonstrated that aberrant m5C modifications across multiple genes are associated with cancer progression [9–11]. Notably,

the RNA methyltransferase Aly/REF export factor (*ALYREF*), a nuclear protein that specifically binds to m5C-modified RNA sites, facilitates the nuclear-to-cytoplasmic export of these modified RNAs, thereby influencing gene expression dynamics [12]. Our preliminary investigations have suggested that *ALYREF* holds potential as a biomarker in localized PCa [9]. However, a comprehensive understanding of its role across the spectrum from early- to late-stage PCa remains elusive. This study aims to address this knowledge gap by elucidating the functional significance of *ALYREF* in PCa progression.

2. Materials and methods

2.1 Public datasets processing

To investigate gene expression patterns, mRNA expression profiles from healthy human tissues were acquired from the Genotype-Tissue Expression (GTEx) database. RNA-sequencing (RNA-seq) data, alongside corresponding clinical annotations for 32 tumor types, were sourced from the UCSC Xena platform. PCa datasets, specifically The Cancer Genome Atlas Prostate Adenocarcinoma (TCGA-PRAD) and SU2C, were obtained from the PCaDB repository, with detailed data processing methodologies described in our previously published work [13]. Additionally, mutational data for the PCa datasets were retrieved from the cBioPortal platform (www.cbioportal.org). Detailed baseline data for all patients are provided in **Supplementary Tables 1,2**.

2.2 Survival analysis

To assess the prognostic relevance of *ALYREF* in PCa patients, we performed Kaplan-Meier (KM) survival analysis alongside Cox proportional hazards regression analyses using the R package survival (version 3.7-0). The optimal threshold for *ALYREF* expression was established with the R package survminer (version 0.5.0), enabling stratification of each cohort into high- and low-expression groups based on this cut-off value.

2.3 *In vitro* validation of *ALYREF* gene dependency

To investigate the dependency of various tumor cell lines on *ALYREF*, we leveraged Clustered Regularly Interspaced Short Palindromic Repeats (CRISPR)-based gene editing data obtained from the Broad Institute's Dependency Map (DepMap) portal (https://depmap.org/portal/). The specific scores for cell lines are summarized in **Supplementary Table 3**. Specifically, we analyzed the Perturbation Effects module within the DepMap framework, which enabled a comprehensive evaluation of *ALYREF*'s role in mediating tumor cell viability and proliferation.

2.4 Mutational profiling

Mutational landscapes in PCa were characterized using the R package Maftools (version 2.22.0) [14]. Variations in mutation frequencies across groups were assessed through the Wilcoxon rank-sum test to identify significant differences. Visualization of the mutational data was performed using the R package ComplexHeatmap (version 2.22.0) to generate comprehensive graphical representations [15].

2.5 Functional enrichment

To explore the associations between *ALYREF* and other mRNAs, we conducted Spearman correlation analysis using the TCGA-PRAD and SU2C datasets, ranking genes by their correlation coefficients in descending order. To identify significantly enriched biological pathways, Gene Set Enrichment Analysis (GSEA) was performed utilizing the R package clusterProfiler (version 4.15.2), focusing on HALLMARK gene sets [16]. The resulting GSEA outputs were visualized using the R package GseaVis (version 0.1.1) to generate clear and informative graphical representations [17].

2.6 Cell assays

The LNCaP and enzalutamide-resistant LNCaP (LNCaP_ENZR) cell lines were sourced and established as previously described [18]. Both cell lines were maintained in Roswell Park Memorial Institute 1640 (RPMI-1640) medium supplemented with 10% fetal bovine serum and 1% penicillin-streptomycin, cultured at 37 °C in a humidified atmosphere with 5% CO_2. Small interfering RNAs (siRNAs) and short hairpin RNAs (shRNAs) targeting *ALYREF* were designed and synthesized by Tsingke Company, with sequences detailed in **Supplementary Table 4**. Transfection protocols and quantitative Polymerase Chain Reaction (qPCR) analyses were conducted following the methodologies outlined in our prior work [19]. To evaluate cell viability and proliferative capacity, Cell Counting Kit-8 (CCK-8) and plate colony formation assays were performed on LNCaP and LNCaP_ENZR cells, with experimental procedures detailed in our previous study [18]. Briefly, cell viability was evaluated using the CCK-8 assay. Transfected cells (1×10^3 per well) were seeded into 96-well plates, and absorbance at 450 nm was measured at 24–72 hours after 2-hour incubation with CCK-8 (MA0218, Meilunbio, Dalian, China). For colony formation, 5×10^3 transfected cells were plated in 6-well plates and cultured for 14 days, after which colonies were fixed, crystal violet-stained, imaged, and counted.

2.7 Statistical analysis

Data processing and graphical representations were conducted using R software (version 4.4.1) alongside GraphPad Prism (version 9.0; GraphPad Software, San Diego, CA, USA). To evaluate associations between variables, Spearman's rank correlation coefficient was computed. Comparisons of continuous variables were performed using either the Wilcoxon rank-sum test or Student's *t*-test, depending on data distribution. Statistical significance was determined using a two-tailed *p*-value threshold of less than 0.05.

3. Results

3.1 Pan-cancer analysis of *ALYREF* expression and prognostic value

To investigate the expression patterns of *ALYREF*, we initially analyzed datasets from the Genotype-Tissue Expression (GTEx) and Human Protein Atlas (HPA) repositories, which provide comprehensive profiles of normal human tissues. As depicted in Fig. 1A, the highest levels of *ALYREF* expression were observed in skeletal muscle, testis, and bladder, while the lowest expression was found in kidney, cervix, and breast tissues, indicating ubiquitous yet variable expression across different organs. By integrating GTEx normal tissue data with TCGA pan-cancer dataset, we observed significantly elevated *ALYREF* expression in cancerous tissues compared with their normal counterparts across most cancer types, with the exception of kidney chromophobe carcinoma (KICH), as shown in Fig. 1B. These differences were statistically significant in the majority of cases. Similarly, when comparing tumor tissues with adjacent non-cancerous tissues in the TCGA pan-cancer cohort, *ALYREF* expression was consistently higher in tumors, except in thyroid carcinoma (THCA) and KICH (Fig. 1C). Furthermore, an analysis of four distinct prognostic endpoints in the TCGA pan-cancer cohort revealed that elevated *ALYREF* expression was associated with unfavorable prognosis in most cancer types, with the notable exception of ovarian cancer (OV), where it appeared to confer a protective effect (Fig. 1D,E). These findings underscore the potential of *ALYREF* as a biomarker in oncology, particularly given its statistically significant differential expression in PCa, highlighting its prognostic relevance across diverse malignancies.

3.2 Prognostic value of *ALYREF* in localized and advanced PCa

To elucidate the prognostic significance of *ALYREF* across different stages of PCa, we analyzed two representative datasets: TCGA-PRAD for localized PCa and SU2C for advanced PCa. As illustrated in Fig. 2A–C, using biochemical recurrence (BCR) in TCGA-PRAD and progression-free survival (PFS) and overall survival (OS) in SU2C as prognostic endpoints, patients with high *ALYREF* expression exhibited significantly worse outcomes. Specifically, in localized PCa, elevated *ALYREF* expression was associated with a higher incidence of biochemical recurrence, while in advanced PCa, it correlated with increased resistance to androgen receptor signaling inhibitors (ARSI) and reduced survival time. Subsequent univariate and multivariate Cox regression analyses further showed that *ALYREF* serves as an independent prognostic risk factor in both localized and advanced PCa (Fig. 2D,E). The results above highlight the prognostic value of *ALYREF* in different stages of PCa.

3.3 *ALYREF* promotes proliferation in multiple tumor cell lines

To investigate the functional role of *ALYREF* following its established prognostic significance, we examined its impact in various cell lines using the DepMap database. By categorizing cell lines according to organ-specific tissue types, we observed that *ALYREF* dependency scores were consistently below 0, with the majority falling below −1 (Fig. 3A). This finding suggests that *ALYREF* is essential for the proliferation of diverse cell lines, particularly cancer cells. Additionally, we ranked cell lines based on their dependency scores from lowest to highest, identifying the top 10 cell lines with the strongest dependency on *ALYREF*. Notably, the breast cancer cell line MDAMB361 exhibited the highest dependency (Fig. 3B). Similarly, among PCa cell lines, the 22RV1 cell line ranked first in terms of dependency score (Fig. 3C). These results underscore the potential of *ALYREF* as a therapy target in cancers.

3.4 Wet-lab validation of *ALYREF* in PCa

To validate the expression dynamics of *ALYREF* across different stages of PCa, we analyzed the TCGA-PRAD, Taylor dataset and GSE35988. These datasets demonstrated that *ALYREF* expression was lowest in benign prostate tissue, elevated in primary PCa, and highest in advanced stages (Fig. 4A). Immunohistochemistry (IHC) results from the Human Protein Atlas (HPA) further revealed that *ALYREF* is predominantly localized in the cytoplasm, cell membrane, and nucleus of PCa tissues (Fig. 4B). To investigate the oncogenic role of *ALYREF* in PCa, we conducted in vitro loss-of-function experiments using wild-type LNCaP (LNCaP_WT) and enzalutamide-resistant LNCaP (LNCaP_ENZR) cell lines. We designed two siRNA sequences targeting *ALYREF*, which effectively reduced *ALYREF* expression (Fig. 4C). CCK-8 assays demonstrated that *ALYREF* knockdown significantly decreased cell viability in both LNCaP_WT and LNCaP_ENZR (Fig. 4D). We further applied stable *ALYREF* knockdown using *ALYREF*-targeting shRNA, and the knockdown efficiency of shRNA was validated (**Supplementary Fig. 1**). Stable *ALYREF* depletion markedly reduced the colony-forming capacity of both LNCaP_WT and LNCaP_ENZR cells (Fig. 4E). These findings indicate that *ALYREF* expression increases with PCa progression and exerts an oncogenic effect.

3.5 Potential biological functions of *ALYREF* in PCa

To elucidate the potential biological functions of *ALYREF* across different stages of PCa, we performed functional enrichment analysis using the TCGA-PRAD and SU2C datasets, prioritizing the top 10 statistically significant pathways (**Supplementary Table 5**). In the TCGA-PRAD dataset (Fig. 5A), activated pathways included Oxidative Phosphorylation, MYC Targets V1, DNA Repair, and MYC Targets V2. These findings suggest that *ALYREF* may promote tumor cell proliferation and survival by enhancing oxidative phosphorylation metabolism, MYC-mediated transcriptional activation, and DNA damage repair mechanisms. Conversely, suppressed pathways encompassed UV Response DN, Mitotic Spindle, Protein Secretion, Epithelial-Mesenchymal Transition, Androgen Response, and KRAS Signaling UP.

In the SU2C advanced PCa dataset (Fig. 5B), the *ALYREF*-associated pathways exhibited similarities to those in TCGA-PRAD. Activated pathways included E2F Targets, G2M Checkpoint, MYC Targets V1, Mitotic Spindle, Unfolded Protein Response, Oxidative Phosphorylation,

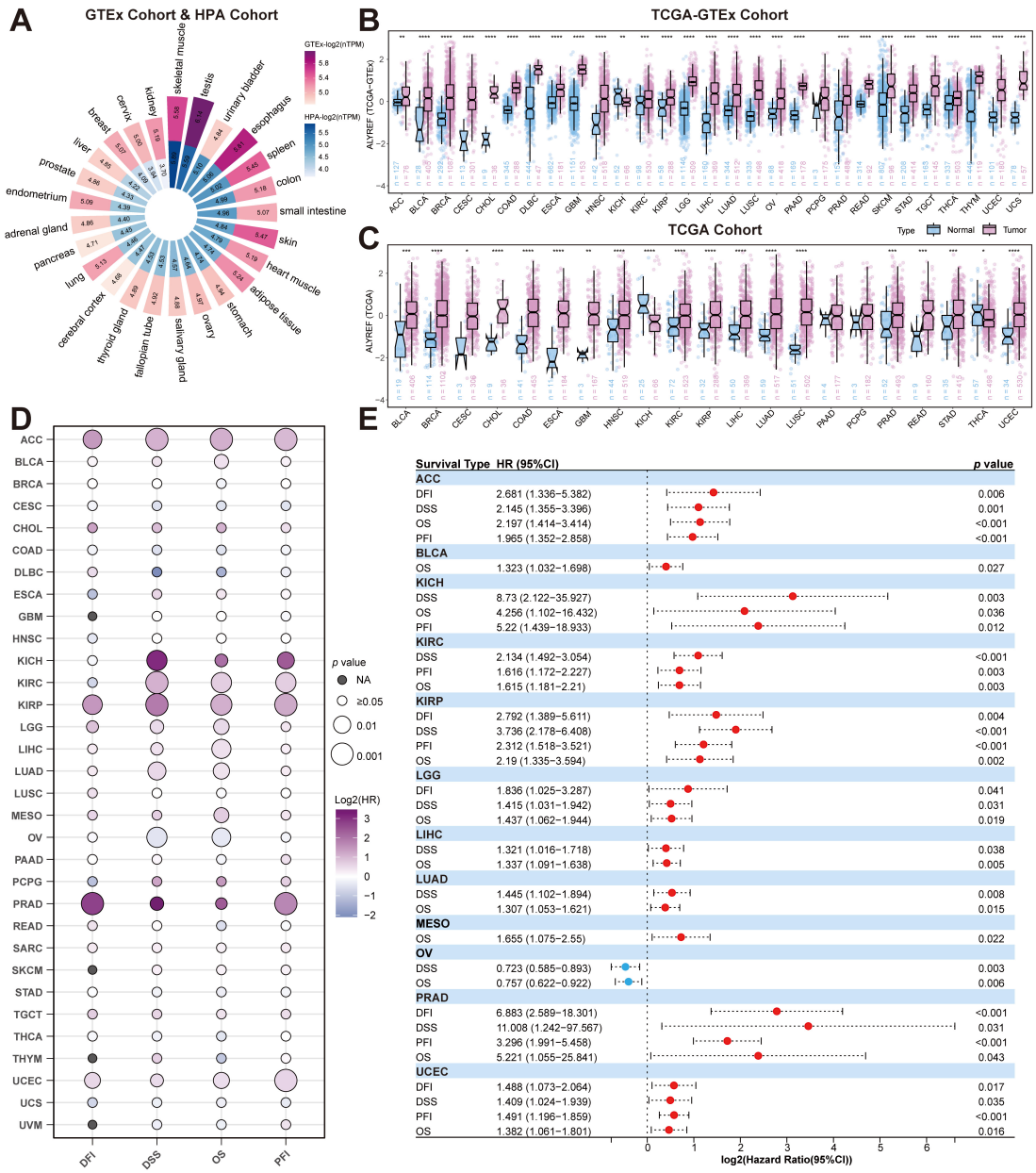

FIGURE 1. Pan-cancer analysis of *ALYREF* expression and prognostic significance. (A) Circular heatmap illustrating the mRNA expression levels of *ALYREF* across various normal human tissues. (B) Boxplot comparing *ALYREF* expression between tumor and normal tissues. (C) Boxplot depicting *ALYREF* expression in tumor versus adjacent non-cancerous tissues. (D) Dot plot representing hazard ratios (HR) with 95% confidence intervals (CI) for *ALYREF* expression across four prognostic endpoints. (E) Forest plot summarizing survival analysis results, including hazard ratios (HR) with 95% CI and *p*-values for each cancer type, with red dots indicating statistical significance ($p < 0.05$). ACC: Adrenocortical carcinoma; BLCA: Bladder urothelial carcinoma; BRCA: Breast invasive carcinoma; CESC: Cervical squamous cell carcinoma and endocervical adenocarcinoma; CHOL: Cholangiocarcinoma; COAD: Colon adenocarcinoma; DLBC: Diffuse large B-cell lymphoma; ESCA: Esophageal carcinoma; GBM: Glioblastoma multiforme; HNSC: Head and neck squamous cell carcinoma; KICH: Kidney chromophobe; KIRC: Kidney renal clear cell carcinoma; KIRP: Kidney renal papillary cell carcinoma; LGG: Lower grade glioma; LIHC: Liver hepatocellular carcinoma; LUAD: Lung adenocarcinoma; LUSC: Lung squamous cell carcinoma; MESO: Mesothelioma; OV: Ovarian serous cystadenocarcinoma; PAAD: Pancreatic adenocarcinoma; PCPG: Pheochromocytoma and paraganglioma; PRAD: Prostate adenocarcinoma; READ: Rectum adenocarcinoma; SARC: Sarcoma; SKCM: Skin cutaneous melanoma; STAD: Stomach adenocarcinoma; TGCT: Testicular germ cell tumors; THCA: Thyroid carcinoma; THYM: Thymoma; UCEC: Uterine corpus endometrial carcinoma; UCS: Uterine carcinosarcoma; UVM: Uveal melanoma; OS: Overall survival; DSS: Disease-specific survival; DFI: Disease-free interval; PFS: Progression-free survival; TCGA: The Cancer Genome Atlas; GTEx: Genotype-Tissue Expression.

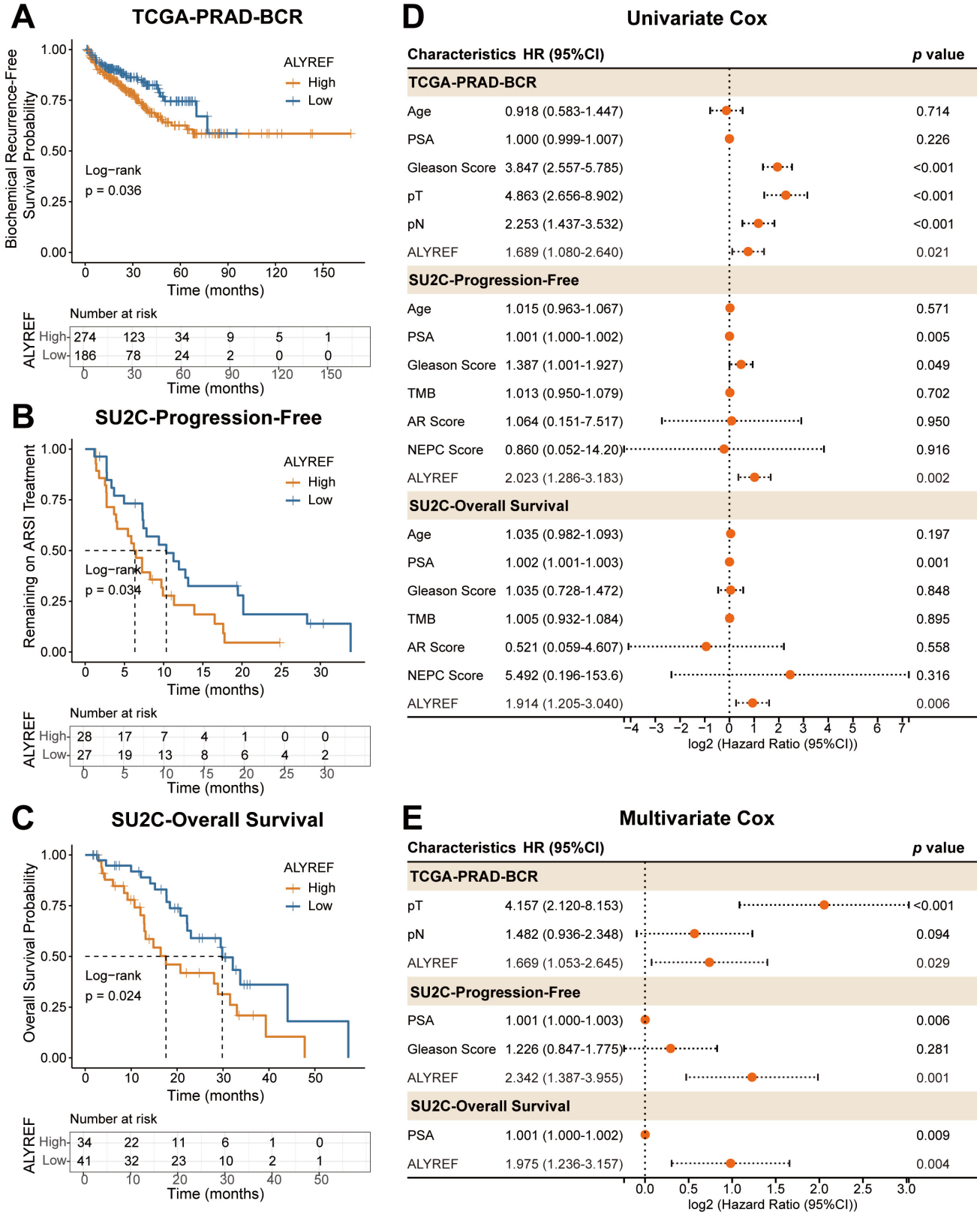

FIGURE 2. Prognostic implications of *ALYREF* in localized and advanced prostate cancer. (A) Kaplan-Meier survival analysis illustrating biochemical recurrence (BCR)-free survival in the TCGA-PRAD cohort. (B) Kaplan-Meier curve depicting progression-free survival (PFS) in the SU2C advanced prostate cancer cohort, stratified by high and low *ALYREF* expression. (C) Kaplan-Meier analysis of overall survival (OS) in the SU2C cohort. (D) Forest plot of univariate Cox proportional hazards regression models evaluating the prognostic impact of clinical characteristics. (E) Forest plot of multivariate Cox proportional hazards regression. ARSI: Androgen Receptor Signaling Inhibitors; PSA: Prostate-Specific Antigen; PRAD: Prostate adenocarcinoma; TCGA: The Cancer Genome Atlas; HR: hazard ratios; CI: confidence intervals; AR: Androgen receptor; NEPC: Neuroendocrine prostate cancer; TMB: Tumor mutational burden; SU2C: Stand Up To Cancer.

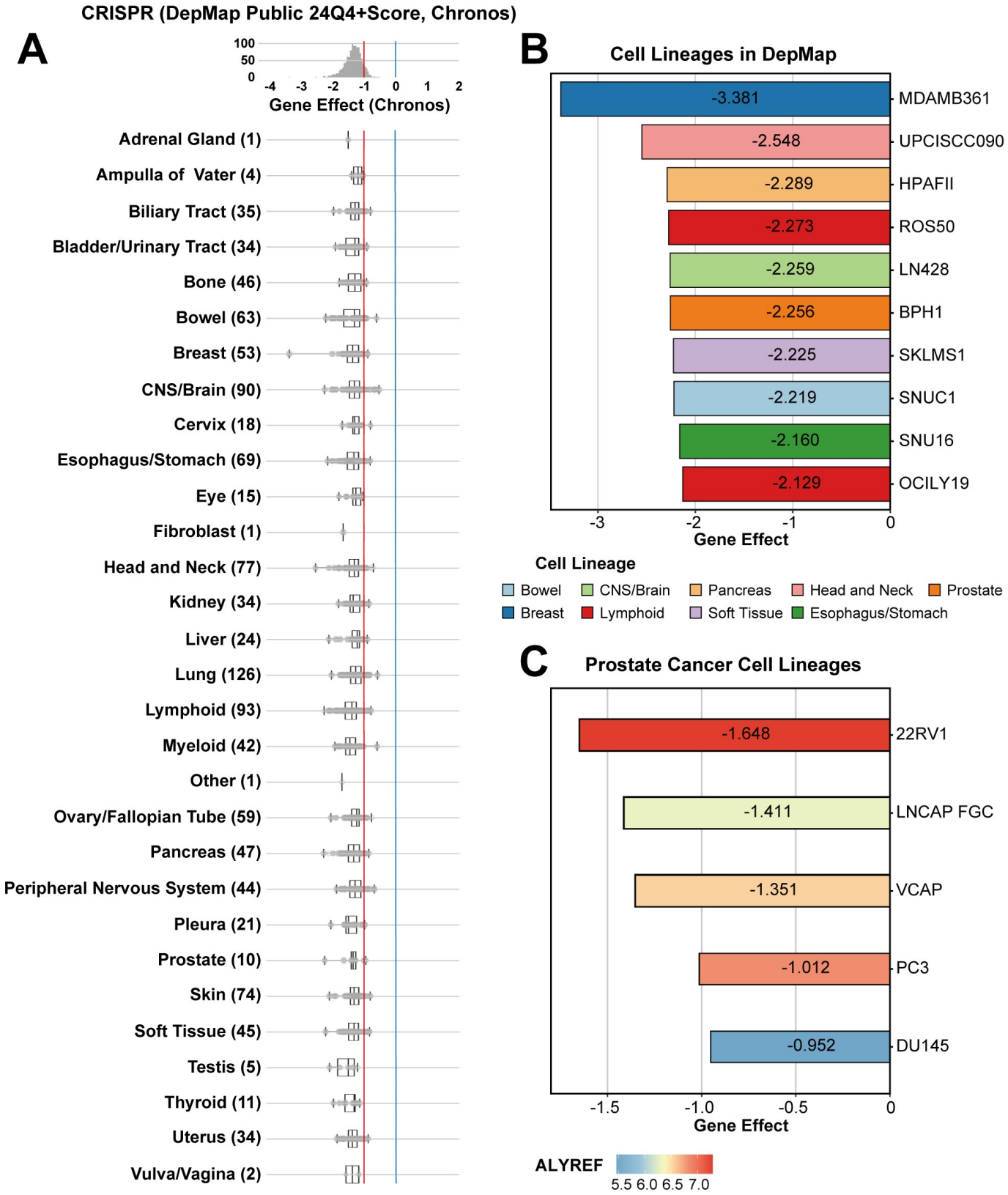

FIGURE 3. Functional dependency of *ALYREF* across tumor cell lines. (A) Boxplot illustrating the distribution of *ALYREF* gene effect scores (Chronos) across various tissue types from the CRISPR (DepMap Public 24Q4+Score, Chronos) dataset, with the vertical dashed line indicating the median gene effect score, highlighting tissue-specific dependency patterns. (B) Bar chart ranking the top 10 cell lines with the strongest *ALYREF* dependency based on gene effect scores across diverse lineages. (C) Bar chart depicting *ALYREF* dependency scores for prostate cancer cell lines. DepMap: Cancer Dependency Map.

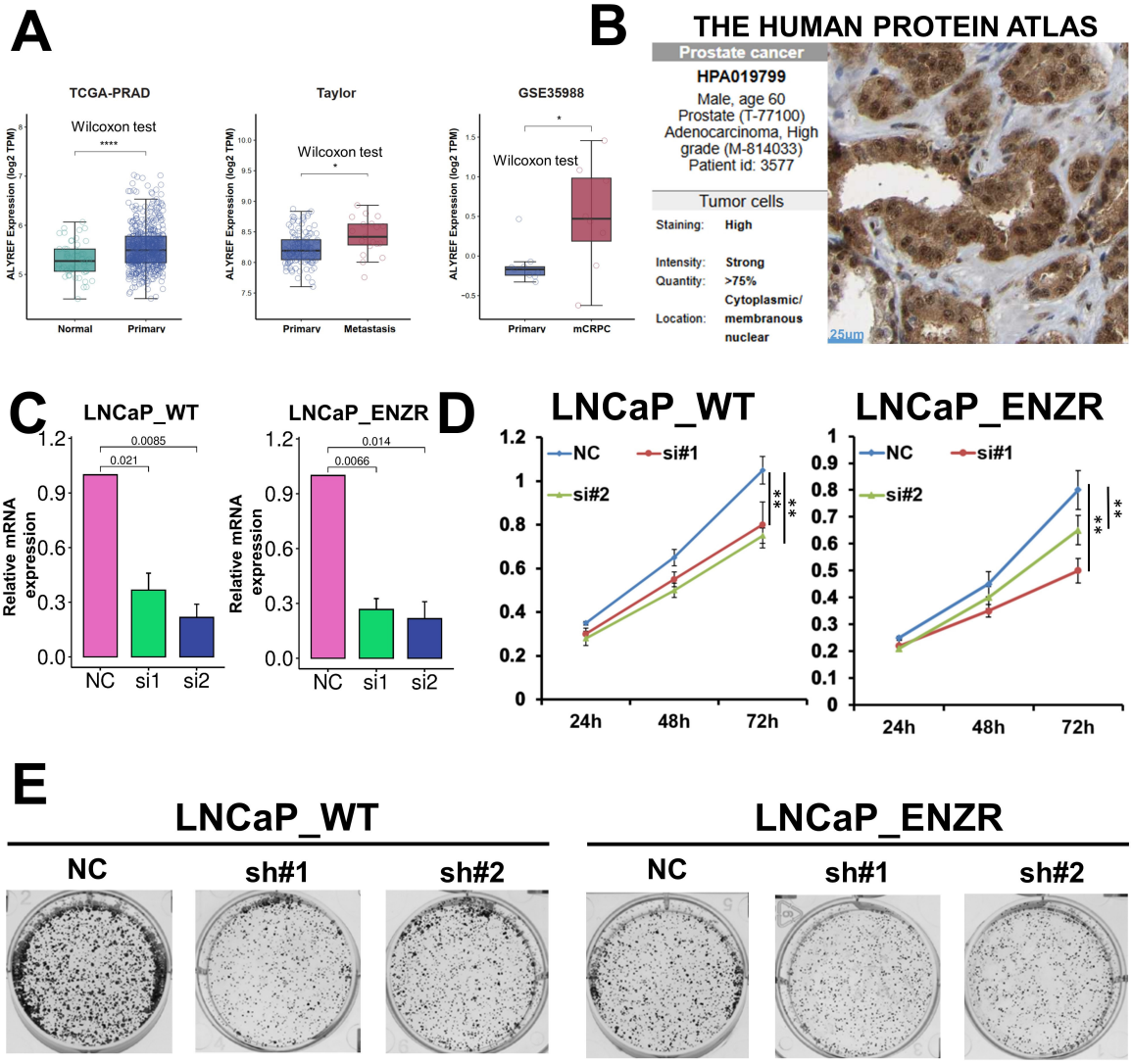

FIGURE 4. Validation of *ALYREF* expression and functional role in prostate cancer. (A) Boxplots comparing *ALYREF* mRNA expression across benign, primary, and advanced prostate cancer stages. (B) Immunohistochemistry (IHC) images from the Human Protein Atlas (HPA) showing *ALYREF* protein expression in prostate tissue. (C) Bar graph depicting relative *ALYREF* mRNA expression in LNCaP wild-type (LNCaP_WT) and enzalutamide-resistant (LNCaP_ENZR) cell lines following transfection with negative control (NC) siRNA or two *ALYREF*-targeting siRNAs (si#1, si#2), with statistical significance indicated. (D) Growth curves from CCK-8 assays showing cell viability over 72 hours in LNCaP_WT and LNCaP_ENZR cells transfected with NC siRNA or *ALYREF*-targeting siRNAs, demonstrating reduced proliferation upon knockdown. (E) Representative images of colony formation assays in LNCaP_WT and LNCaP_ENZR cells transfected with NC shRNA or two *ALYREF*-targeting shRNAs (sh#1, sh#2). NC: negative control. (*$p < 0.05$, **$p < 0.01$, ****$p < 0.0001$).

UV Response UP, and MTORC1 Signaling. These results indicate that *ALYREF* may drive tumor progression by activating the E2F transcriptional network, regulating the G2M checkpoint, facilitating mitotic processes, modulating the unfolded protein response, and enhancing MTORC1 signaling, thereby supporting cell cycle progression, protein homeostasis, and metastatic tumor resistance. The DNA Repair pathway showed a weaker association. Notably, only one pathway, KRAS Signaling DN, was suppressed in the SU2C dataset. These findings suggest that *ALYREF* is associated with partially overlapping activated pathways across different stages of PCa, with some distinct differences potentially linked to the previously observed increase in *ALYREF* expression during PCa progression.

3.6 *ALYREF* and genetic mutations in PCa

To comprehensively explore the association between *ALYREF* and genetic mutations in PCa, we conducted a multi-omics analysis. In localized PCa, the mutational burden was relatively low, with genes such as Tumor Protein p53 (*TP53*), Speckle-Type POZ Protein (*SPOP*), and Titin (*TTN*) exhibiting mutation frequencies ≥10%, as shown in Fig. 6A. When stratifying by *ALYREF* expression levels, we observed significantly higher mutation frequencies for TP53 and LRP1B in the high *ALYREF* expression group (Fig. 6B). Conversely, when grouping by mutation status, only LRP1B mutations were associated with a statistically significant increase in *ALYREF* expression (Fig. 6C). In advanced PCa cohorts, the mutational burden was

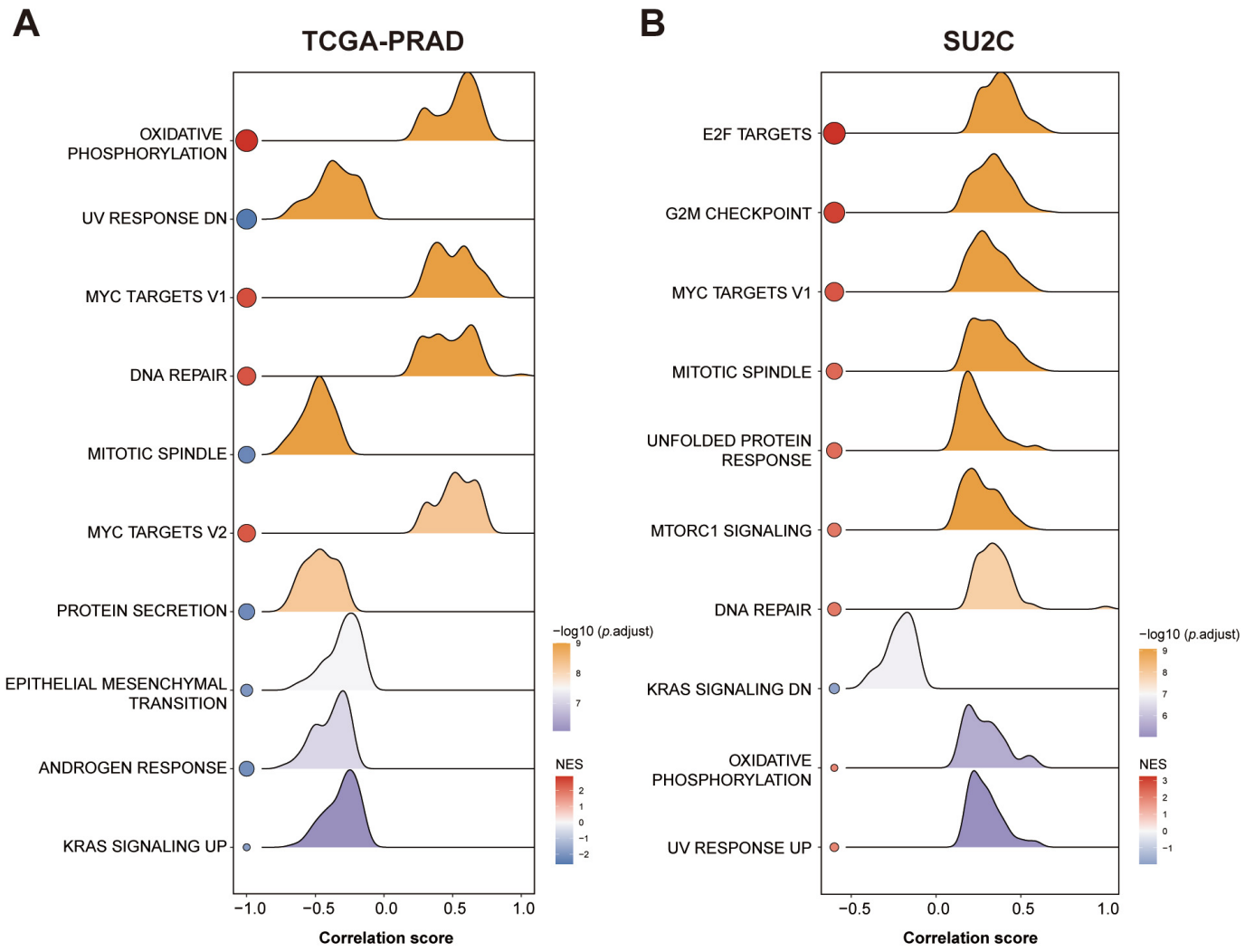

FIGURE 5. Functional enrichment analysis of *ALYREF*-associated pathways in prostate cancer. (A) Gene Set Enrichment Analysis (GSEA) plot for the TCGA-PRAD cohort, displaying the top 10 significantly enriched pathways ranked by *p* value. (B) GSEA plot for the SU2C cohort, highlighting the top 10 enriched pathways ranked by *p* value. TCGA-PRAD: The Cancer Genome Atlas Prostate Adenocarcinoma; SU2C: Stand Up To Cancer.

markedly elevated, with TP53 and TTN mutations occurring at frequencies ≥30%, and AR mutations at 19% (Fig. 6D). Upon further analysis of *ALYREF* expression subgroups, only SYNE1 displayed a significantly higher mutation frequency in the high *ALYREF* expression group, while TP53 mutations showed a modestly elevated frequency (Fig. 6E). Intriguingly, when stratified by the mutation status of high-frequency mutated genes, *ALYREF* expression levels remained largely unchanged (Fig. 6F). These findings suggest that *ALYREF* expression subgroups exhibit distinct patterns of genetic mutation heterogeneity. However, *ALYREF* expression appears relatively stable in both localized and advanced PCa, with minimal variation driven by genetic mutations in most cases.

4. Discussion

Localized PCa is typically characterized by an indolent clinical course, with many patients exhibiting no noticeable symptoms or only mild manifestations that may resemble benign prostatic hyperplasia [20]. In some instances, the disease remains undetected during a patient's lifetime and is identified only posthumously during autopsy. However, once PCa progresses to an advanced stage, the prognosis becomes significantly worse, often accompanied by resistance to multiple therapeutic interventions [21]. For patients with advanced PCa, particularly those with metastatic disease, ARSI therapy remains the standard first-line treatment. However, the development of resistance is almost inevitable [22]. At present, treatment response is primarily assessed through rising Prostate-Specific Antigen (PSA) levels and imaging evaluations, such as Computed Tomography (CT) and bone scans, yet these approaches still lack sufficient specificity [23]. Consequently, the development of novel biomarkers and therapy targets is critical for improving the management and outcomes of PCa across its continuum.

ALYREF, a heat-stable nuclear protein, exhibits a distinctive capacity to recognize m5C sequences and function as a molecular chaperone [24]. This protein plays a critical role in facilitating the dimerization of unfolded leucine zipper motifs, thereby promoting transcriptional activation [25]. Additionally, *ALYREF* interacts with specific sequences in the translational regions of mRNAs, modulating gene expres-

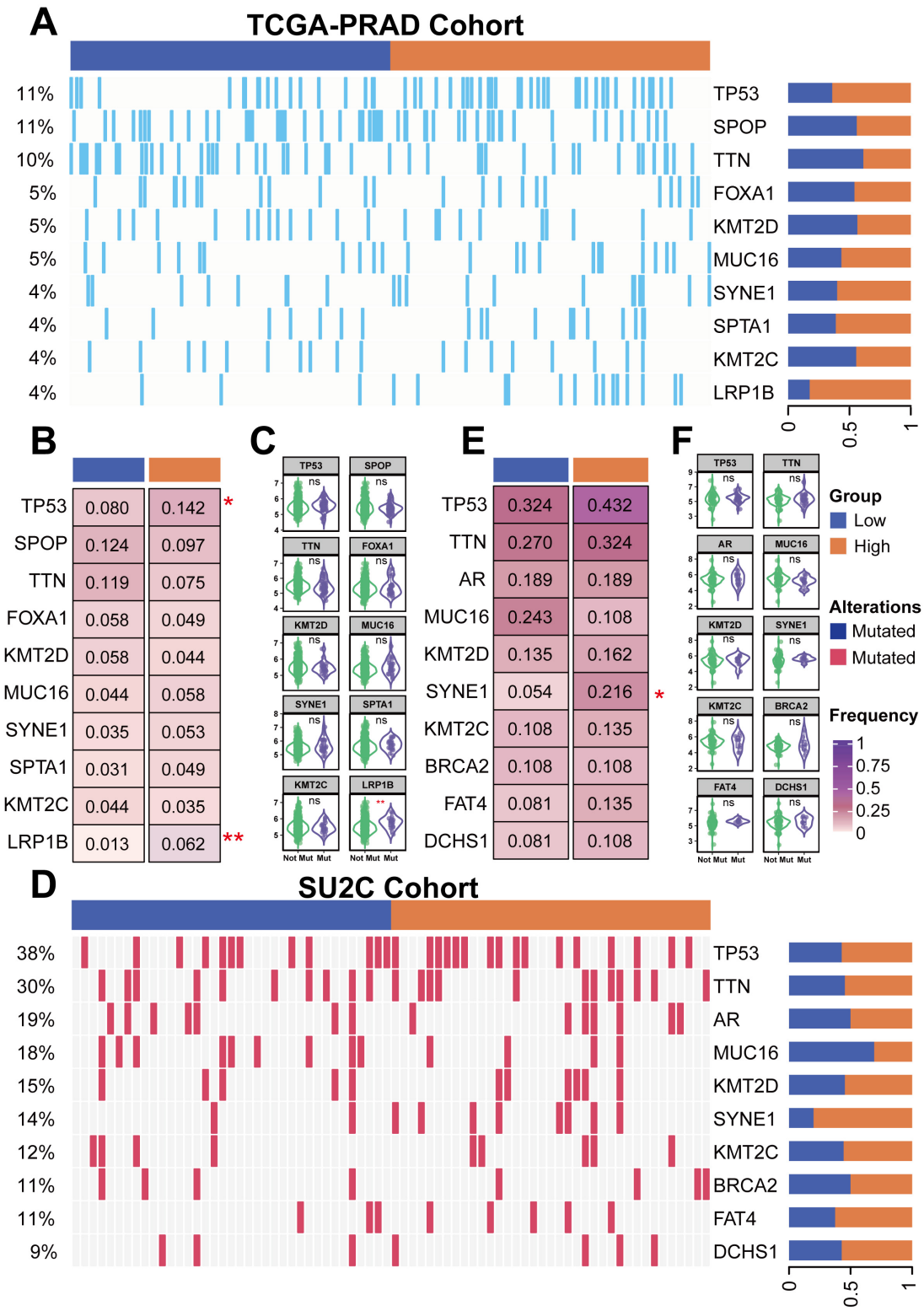

FIGURE 6. Mutational landscape and association with *ALYREF* expression in prostate cancer. (A) Oncoplot displaying the mutation frequency of the top 10 most frequently mutated genes in the TCGA-PRAD cohort. (B) Boxplot comparing mutation frequencies of selected genes between high and low *ALYREF* expression groups in the TCGA-PRAD cohort, with statistical significance denoted by asterisks (*$p < 0.05$, **$p < 0.01$). (C) Boxplot illustrating *ALYREF* expression levels stratified by mutation status (mutated *vs.* non-mutated) for key genes in the TCGA-PRAD cohort. (D) Oncoplot showing the mutation frequency of the top 10 most frequently mutated genes in the SU2C cohort. (E) Boxplot comparing mutation frequencies of selected genes between high and low *ALYREF* expression groups in the SU2C cohort, with significant differences marked. (F) Boxplot depicting *ALYREF* expression levels stratified by mutation status for key genes in the SU2C cohort. TCGA-PRAD: The Cancer Genome Atlas Prostate Adenocarcinoma; SU2C: Stand Up To Cancer.

sion, nuclear mRNA export, and genomic stability [24, 26]. Emerging evidence has implicated *ALYREF* in tumorigenesis across various cancer types. For instance, Nan *et al.* [27] demonstrated that *ALYREF*, through its interaction with modified circular RNA ras-responsive element-binding protein 1 (*circRREB1*), enhances lung cancer progression by inducing mitophagy. Furthermore, *ALYREF* has been shown to stabilize Cell-cycle related and expression-elevated protein (CREPT) mRNA, thereby promoting nasopharyngeal carcinoma progression [28], and to modify Metastasis-associated lung adenocarcinoma transcript 1 (*MALAT1*), contributing to sorafenib resistance in hepatocellular carcinoma [29]. The advent of multi-omics technologies has accelerated the discovery of novel cancer biomarkers [30–32]. Leveraging multi-omics data, this study elucidates the pivotal role of *ALYREF* in the progression of PCa from early to advanced stages.

Our pan-cancer analysis aligns with previous studies, confirming that *ALYREF* is overexpressed in most tumor types and serves as an unfavorable prognostic factor. This pattern is particularly pronounced in PCa, where elevated *ALYREF* expression correlates with adverse outcomes across early-stage BCR and late-stage PFS and OS. Additionally, pan-cancer CRISPR screening data indicate that *ALYREF* is essential for the survival of most tumor cells. Consistent with these findings, *in vitro* experiments using PCa cell models, specifically LNCaP_WT and LNCaP_ENZR, demonstrate that *ALYREF* knockdown significantly attenuates PCa progression.

While our study has established that *ALYREF* promotes the progression of PCa across different stages, the mechanisms underlying its role remain elusive. Recent research has revealed that *ALYREF* interacts with m5C-modified Acetyl-CoA carboxylase 1 (*ACC1*) mRNA, enhancing its stability and nuclear export, which in turn upregulates ACC1 expression and lipid accumulation, thereby driving PCa progression [33]. However, similar to other studies on *ALYREF*, this work focuses on *ALYREF*'s auxiliary role in tumor progression, such as stabilizing RNA and facilitating nuclear export, without positioning *ALYREF* as the central focus of investigation, particularly in the context of PCa. Our functional enrichment analysis demonstrates that *ALYREF* is associated with several consistently activated pathways in both early- and late-stage PCa, including Oxidative Phosphorylation, MYC Targets V1, and DNA Repair. These findings suggest a multifaceted role for *ALYREF* in PCa biology. Meanwhile, with the rapid advancement of urine-based biomarkers as a non-invasive diagnostic approach, the relevance of *ALYREF* in this context warrants attention. Garcia-Martin *et al.* [34] reported that *ALYREF* is a key RNA-binding protein recognizing exosomal EXOmotifs and regulating the selective loading of specific molecules into small extracellular vesicles. This mechanism suggests that *ALYREF* may influence the release of cellular components into urine. Future studies are warranted to elucidate the mechanistic details of how *ALYREF* drives PCa progression across its various stages, building on these preliminary insights.

Several limitations should be acknowledged. This study relied mainly on publicly available datasets, which may introduce data heterogeneity. Moreover, investigations of *ALYREF* were limited to *in silico* and *in vitro* analyses, and further *in vivo* and mechanistic studies are needed to fully elucidate its biological functions.

5. Conclusions

ALYREF is overexpressed in PCa tissues, correlating with adverse outcomes. Besides, following the knockdown of *ALYREF*, the progression of PCa and its resistance to treatment are attenuated. In summary, *ALYREF* emerges as a promising biomarker and therapeutic target, necessitating further mechanistic studies for personalized PCa strategies.

AVAILABILITY OF DATA AND MATERIALS

All data used in this study were obtained from publicly available databases. Detailed information on the datasets is provided in the Materials and Methods section.

AUTHOR CONTRIBUTIONS

ZDC, YL, LZ, SDS and JML—were responsible for data collection and analysis. ZDC, YL and CFZ—conducted the cell experiments. ZDC, YL and SDS—drafted the initial manuscript. JHC, CC, YRZ and WDZ—contributed to the revision of the manuscript. JHC, YRZ and WDZ—provided funding for the project. YRZ and WDZ—supervised and designed the study. All authors contributed to the revision of the manuscript and approved the final version.

ETHICS APPROVAL AND CONSENT TO PARTICIPATE

Not applicable.

ACKNOWLEDGMENT

We express our gratitude to the creators of the publicly accessible datasets and the developers of the R-based bioinformatics tools utilized in this research.

FUNDING

This work was supported by the Guangzhou Health Science and Technology Project (20251A011001), Science and Technology Project of Guangzhou (2024A03J1108), National Natural Science Foundation of China (82573325), the Regional Joint Fund—Regional Cultivation Project (Grant number 2023A1515140040) and Guangdong S&T Program (2023B1111030006).

CONFLICT OF INTEREST

The authors declare no conflict of interest.

SUPPLEMENTARY MATERIAL

Supplementary material associated with this article can be found, in the online version, at https://oss.jomh.org/

files/article/2049382999391125504/attachment/Supplementary%20material.xls.

REFERENCES

[1] Bray F, Laversanne M, Sung H, Ferlay J, Siegel RL, Soerjomataram I, *et al.* Global cancer statistics 2022: GLOBOCAN estimates of incidence and mortality worldwide for 36 cancers in 185 countries. CA: A Cancer Journal for Clinicians. 2024; 74: 229–263.

[2] Cornford P, van den Bergh RCN, Briers E, Van den Broeck T, Brunckhorst O, Darraugh J, *et al.* EAU-EANM-ESTRO-ESUR-ISUP-SIOG guidelines on prostate cancer—2024 update. Part I: screening, diagnosis, and local treatment with curative intent. European Urology. 2024; 86: 148–163.

[3] Yin W, Chen G, Li Y, Li R, Jia Z, Zhong C, *et al.* Identification of a 9-gene signature to enhance biochemical recurrence prediction in primary prostate cancer: a benchmarking study using ten machine learning methods and twelve patient cohorts. Cancer Letters. 2024; 588: 216739.

[4] Liu D, Wang L, Guo Y. Advances in and prospects of immunotherapy for prostate cancer. Cancer Letters. 2024; 601: 217155.

[5] Chen Y, Long T, Wang M, Liu S, Lv Z, Jiang Y, *et al*. Prospective cohort study integrating plasma proteomics and machine learning for early risk prediction of prostate cancer. International Journal of Surgery. 2025; 111: 6123–6134.

[6] Li C, Wu L, Zhong B, Gan Y, Zhou L, Tan S, *et al.* Integrated multi-omics profiling of immune microenvironment and drug resistance signatures for precision prognosis in prostate cancer. Cancer Drug Resistance. 2025; 8: 31.

[7] Hanahan D. Hallmarks of cancer: new dimensions. Cancer Discovery. 2022; 12: 31–46.

[8] Liu WW, Zheng SQ, Li T, Fei YF, Wang C, Zhang S, *et al.* RNA modifications in cellular metabolism: implications for metabolism-targeted therapy and immunotherapy. Signal Transduction and Targeted Therapy. 2024; 9: 70.

[9] Tan X, Cai Z, Chen G, Cai C, Chen J, Liang Y, *et al.* Identification and verification of an ALYREF-involved 5-methylcytosine based signature for stratification of prostate cancer patients and prediction of clinical outcome and response to therapies. Discover Oncology. 2023; 14: 62.

[10] Cai Z, Jiang Z, Li S, Mo S, Wang S, Liang M, *et al.* RNA modification Regulators' Co-Expression Score (RMRCoeS) predicts biochemical recurrence and therapy response in prostate cancer: a multi-omics and experimental validation study. International Immunopharmacology. 2024; 139: 112723.

[11] Wang W, Ding Y, Zhao H, Wang S, Huang J, Sun L. NSUN2-tRNA$^{Val-CAC}$-axis-regulated codon-biased translation drives triple-negative breast cancer glycolysis and progression. Cellular & Molecular Biology Letters. 2025; 30: 100.

[12] Gao X, Shen Y, Xiao Z, Han Z, Liu X, Cai A, *et al.* Preservation of ALYREF phase separation mitigates doxorubicin-induced cardiomyocyte DNA damage and cardiotoxicity. Advanced Science. 2025; 12: e05270.

[13] Li R, Zhu J, Zhong WD, Jia Z. Comprehensive evaluation of machine learning models and gene expression signatures for prostate cancer prognosis using large population cohorts. Cancer Research. 2022; 82: 1832–1843.

[14] Mayakonda A, Lin DC, Assenov Y, Plass C, Koeffler HP. Maftools: efficient and comprehensive analysis of somatic variants in cancer. Genome Research. 2018; 28: 1747–1756.

[15] Gu Z. Complex heatmap visualization. Imeta. 2022; 1: e43.

[16] Xu S, Hu E, Cai Y, Xie Z, Luo X, Zhan L, *et al.* Using clusterProfiler to characterize multiomics data. Nature Protocols. 2024; 19: 3292–3320.

[17] Zhang J, Li H, Tao W, Zhou J. GseaVis: an R package for enhanced visualization of gene set enrichment analysis in biomedicine. Med Research. 2025; 1: 131–135.

[18] Zhong C, Wang J, Peng H, Lu J, Long Z, Lin Z, *et al*. GG-NER's role in androgen receptor signaling inhibitor response for advanced prostate cancer. Cell Communication and Signaling. 2024; 22: 600.

[19] Zhong C, Long Z, Yang T, Wang S, Zhong W, Hu F, *et al.* M6A-modified circRBM33 promotes prostate cancer progression via PDHA1-mediated mitochondrial respiration regulation and presents a potential target for ARSI therapy. International Journal of Biological Sciences. 2023; 19: 1543–1563.

[20] Sartor O. Localized prostate cancer—then and now. The New England Journal of Medicine. 2023; 388: 1617–1618.

[21] Cai M, Song XL, Li XA, Chen M, Guo J, Yang DH, *et al*. Current therapy and drug resistance in metastatic castration-resistant prostate cancer. Drug Resistance Updates. 2023; 68: 100962.

[22] Khorasanchi A, Hong F, Yang Y, Singer EA, Wang P, Li M, *et al.* Overcoming drug resistance in castrate-resistant prostate cancer: current mechanisms and emerging therapeutic approaches. Cancer Drug Resistance. 2025; 8: 9.

[23] Shagera QA, Karfis I, Kristanto P, Spyridon S, Diamand R, Santapau A, *et al.* PSMA PET/CT for response assessment and overall survival prediction in patients with metastatic castration-resistant prostate cancer treated with androgen receptor pathway inhibitors. Journal of Nuclear Medicine. 2023; 64: 1869–1875.

[24] Shi M, Zhang H, Wu X, He Z, Wang L, Yin S, *et al*. ALYREF mainly binds to the 5′ and the 3′ regions of the mRNA *in vivo*. Nucleic Acids Research. 2017; 45: 9640–9653.

[25] Pacheco-Fiallos B, Vorländer MK, Riabov-Bassat D, Fin L, O'Reilly FJ, Ayala FI, *et al.* mRNA recognition and packaging by the human transcription-export complex. Nature. 2023; 616: 828–835.

[26] Fan J, Wang K, Du X, Wang J, Chen S, Wang Y, *et al.* ALYREF links 3′-end processing to nuclear export of non-polyadenylated mRNAs. The EMBO Journal. 2019; 38: e99910.

[27] Cai D, Chen X, Xu H, Zhao Q, Zhou X, Wu J, *et al.* m5C-modified circRREB1 promotes lung cancer progression by inducing mitophagy. Journal of Experimental & Clinical Cancer Research. 2025; 44: 203.

[28] Xu D, Fu Y, Sun H, Lu Y, Shen B, Hao X. ALYREF stabilizes CREPT mRNA to accelerate the development of nasopharyngeal carcinoma through dependence on m5C modification. Experimental Cell Research. 2025; 452: 114747.

[29] Shi CJ, Pang FX, Lei YH, Deng LQ, Pan FZ, Liang ZQ, *et al.* 5-methylcytosine methylation of MALAT1 promotes resistance to sorafenib in hepatocellular carcinoma through ELAVL1/SLC7A11-mediated ferroptosis. Drug Resistance Updates. 2025; 78: 101181.

[30] Cheng J, He Z, Jing J, Liu Y, Zhang H. Integrating machine learning and multi-omics to identify key SUMOylation molecular signature in sarcoma. Life Conflux. 2024; 1: e88.

[31] Huang C, Liu Z, Guo Y, Wang W, Yuan Z, Guan Y, *et al.* scCancerExplorer: a comprehensive database for interactively exploring single-cell multi-omics data of human pan-cancer. Nucleic Acids Research. 2025; 53: D1526–D1535.

[32] Xie J, Xie Y, Tan W, Ye Y, Ou X, Zou X, *et al.* Deciphering the role of *ELAVL1*: insights from pan-cancer multiomics analyses with emphasis on nasopharyngeal carcinoma. Journal of Translational Internal Medicine. 2025; 13: 138–155.

[33] Zhang Y, Chen XN, Zhang H, Wen JK, Gao HT, Shi B, *et al.* CDK13 promotes lipid deposition and prostate cancer progression by stimulating NSUN5-mediated m5C modification of ACC1 mRNA. Cell Death & Differentiation. 2023; 30: 2462–2476.

[34] Garcia-Martin R, Wang G, Brandão BB, Zanotto TM, Shah S, Kumar Patel S, *et al.* MicroRNA sequence codes for small extracellular vesicle release and cellular retention. Nature. 2022; 601: 446–451.

How to cite this article: Zhouda Cai, Yu Liu, Shengda Song, Chuanfan Zhong, Jiahong Chen, Le Zhang, Chao Cai, Jianming Lu, Yanru Zeng, Weide Zhong. *ALYREF* correlates with tumor progression and therapy resistance in localized and advanced prostate cancer. Journal of Men's Health. 2026; 22(4): 42-52. doi: 10.22514/jomh.2026.033.